Shock Vibration Control of Structures using Fluid Viscous Dampers

D. I. Narkhede & R. Sinha
Indian Institute of Technology Bombay, Mumbai-400076, India

15 WCEE
LISBOA 2012

SUMMARY:
Vibration control systems in the form of shock and vibration isolators have been devised to provide dynamic protection to structural systems. Amongst such devices, fluid viscous dampers are found to have desirable performance to control shock loads. Fluid viscous dampers are attractive for enhancing the performance because they not only reduce the deformation demand but also the force transferred to the structure due to energy dissipation. Conventional linear fluid viscous dampers can dissipate only limited amount of energy, and are not as effective as nonlinear dampers for shock loads. This paper experimentally evaluates the performance of such dampers for shock loads, and presents the dynamic behavior of an example system. The mathematical formulation and relative performance of structures subjected to short-duration pulse excitations are discussed. The influence of the damper exponent α and coefficient of damper c_α are also evaluated. The paper also presents some design charts, which can be used for preliminary decision on parameters of nonlinear dampers to be used in design.

Keywords: fluid viscous dampers; energy dissipation; impulse load; shock load.

1. INTRODUCTION

Structural passive control systems primarily include energy dissipation and base isolation devices. A variety of passive energy dissipating devices has been developed during the past two decades such as the metallic dampers, friction dampers, visco-elastic dampers and the fluid viscous dampers. A comprehensive review of passive energy dissipation concepts and application is available in published literature (Soong and Dargush, 1997). The addition of passive energy dissipation devices to structural system reduces the excessive deformation and ductility demand and at the same time enhances its energy dissipation capacity. The passive energy dissipation devices have been found to be effective for both short-duration loads (shock loads) as well as longer-duration loads (earthquake forces or wind loads).

Among the energy dissipation devices, fluid viscous dampers (FVD) have been widely used in vibration control of various structural and mechanical systems. As pure viscous behavior may be achieved by forcing fluid through orifices (where damper force is proportional to velocity), a special role is played by fluid viscous dampers as passive energy dissipation devices (Pekcan et al., 1999, Soong and Dargush, 1997), and can also be utilized in base isolation (Makris, 1992). There are several potential equipment and mechanical systems whose performance can be greatly enhanced by using the right type/configuration of fluid viscous dampers. Fluid viscous dampers are especially attractive for enhancing the performance of structures because they not only reduce the deformation demand but also the force demand.

The damper force of a nonlinear FVD is proportional to a fractional power-law of the velocity, whose exponent ranges between 0.1 and 1.0. The supplemental damping ratio can be obtained by evaluating the equivalence between a nonlinear and a linear fluid viscous damper. The criteria for evaluating the

supplemental damping ratio for a nonlinear fluid viscous damper presented in literature are expressed in terms of energy dissipated (Lin and Chopra, 2002) or power consumption (Peckan et al., 1999).

This paper presents the experimental work performed for modeling of nonlinear FVD subjected to shock excitation. It also discusses the dynamic behavior of single-degree-of-freedom (SDOF) system with linear and nonlinear FVDs when subjected to shock loading. The damping coefficient of damper, c_α for a nonlinear damper is obtained by imposing the equivalence between a nonlinear and a linear fluid viscous damper. The shock spectra for an example pulse loading, which can be used for preliminary design of the dampers, has also been presented.

2. FLUID VISCOUS DAMPERS

2.1. Components

Figure 2.1. shows a longitudinal cross section of a typical fluid viscous damper. It consists of a stainless steel piston, with a bronze orifice head, and a self-contained piston displacement accumulator. The damper is filled with a compressible viscous fluid which is generally non-flammable, non-toxic, environmentally safe, and thermally stable. The dampers output force is resistive; therefore it acts in a direction opposite to that of the input motion. The means of energy dissipation is by heat transfer, i.e., the mechanical energy dissipated by the damper causes a heating of the dampers fluid and mechanical parts, and this thermal energy is transferred to the environment (Constantinou and Symans,1992).
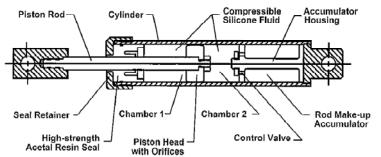
2.2. Operation

Internal force is generated by the fluid damper due to pressure differential across the piston head. During the motion of the piston head, the fluid volume is changed by the product of travel and piston rod area. Since the fluid is compressible, this change in fluid volume is accompanied by the development of a spring like restoring force. This is prevented by the use of the accumulator. At higher frequency, the fluid viscous dampers exhibit strong stiffness. In general, this cutoff frequency depends on the design of the accumulator (Constantinou and Symans,1993).

2.3. Mathematical modeling

Fluid viscous dampers have the unique advantage of reducing the shearing and bending stresses at the same time, as the velocity-dependent maximum damping force is 90 degrees out of phase with the maximum deflection of the structure as shown in Fig. 2.2. In addition, installing FVDs in a structure does not alter its force displacement relationship and hence its dynamic modal characteristics (Martinez-Rodrigo and Romero, 2003). The ideal force output of a nonlinear FVD is proportional to a fractional power-law of the velocity is expressed as:

$$f_D = c_\alpha \, \text{sgn}(\dot{u}) |\dot{u}|^\alpha \tag{2.1}$$

where f_D is the damper force, c_α is the damping coefficient with units of force per velocity raised to the power α, $\dot{u}$ is the relative velocity between the two ends of the damper and $\text{sgn}(\cdot)$ is the signum function. The piston head consists of orifices that are designed with a series of specially shaped passages to alter flow characteristics with fluid speed. A schematic of this orifice is shown in Fig. 2.3. The damper with $\alpha = 1$ is known as linear FVD in which damper force is proportional to the velocity. The damper with $\alpha < 1$ is called a nonlinear FVD. Fig. 2.4. shows the force-velocity relationship of FVD wherein the peak dampers force is limited when velocity exponent is less than 1. This property demonstrates the efficiency of nonlinear FVD ($\alpha < 1$) to limit peak damper force in minimizing high velocity shocks. This behavior is contrary to that of the linear FVD and thus makes the nonlinear FVDs attractive for control of impulse-type or short-duration loads.
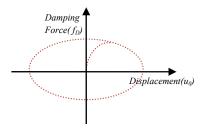
Figure 2.1. Typical longitudinal cross section of a fluid viscous damper (Constantinou and Symans,1992)

Figure 2.2. Idealized force-displacement relationship
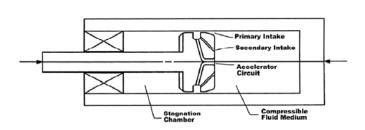

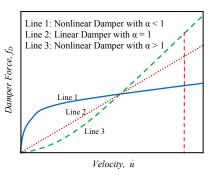**Figure 2.3.** Fluidic control orifice

Figure 2.4. Force-velocity relationship for of fluid viscous dampers

2.4. Applications

(Goel, 2005) and (Lin and Chopra, 2002) have proposed nonlinear FVDs for control of seismic response of SDOF system. Their study showed that nonlinear fluid viscous dampers can achieve essentially the same reduction in response but with significantly reduced damper force compared to linear damper for systems with very short periods. (Dicleli and Mehta, 2007) used Chevron braced frame with nonlinear fluid viscous dampers in the near-fault ground motion with peak ground velocity varying from 0.37 m/sec to 1.7 m/sec and velocity pulse periods varying from 1.1 sec to 5.0 sec. They found that the energy dissipated by the fluid viscous dampers prevented the buckling of braces and causes the frame members to remain within elastic limits. While the aforementioned studies have led to improved understanding of how fluid viscous dampers reduces earthquake-induced deformations, it is also important to understand the response of structure with these dampers to shock environment. In this paper, the use of nonlinear fluid viscous dampers in structural systems subjected to shock environment has been investigated.

3. IMPULSE OR SHOCK LOADS

Many structures are sometimes subjected to relatively large forces suddenly applied over a very short duration of time (impulse or shock loads). For typical shock loading, the force duration is short relative to the natural period of the structure, i.e $t_d/T_n < 1$, where t_d is the duration of loading and T_n is the fundamental time period of the structure. These forces can produce very high response. The maximum amplitude may occur during or after the application of the shock and its magnitude depends on the ratio of duration of the pulse to the natural period of the structure. The impulse often excites several natural frequencies of a complex structure, which may result in large cyclic stresses damaging the structure or impairing its performance. Examples of sources of impulse shock are free-fall impacts, collisions, explosions, gunfire, projectile impacts, high-speed fluid entry, aircraft landing and braking loads, and missile launching and staging (Harris and Crede, 1961).

4. MODELING OF NONLINEAR FVD SUBJECTED TO HALF-CYCLE SINE SHOCK

4.1 Experimental setup

The non-periodic nature of shock is experimentally simulated on a state-of-art shock testing machine as shown in Fig. 4.1. The shock testing machine works on the principle of free fall from a specified drop height thus imparting kinetic energy to the corset side of the machine. The shock is generated by lifting the corset to specified drop height and then releasing it to fall freely under gravity striking the buffer mass with specified rubber thickness interposed between steel plate and the buffer mass. The shock generated as a result of this is a half-cycle sine pulse at the damper fixed end, fitted in the corset assembly. The main purpose of shock tests conducted on the fluid viscous dampers was to measure the shock parameters, the acceleration and duration of the half sine shock pulse as input at the damper fixed end and response as output at the damper piston end. The programme for shock testing of dampers made use of the dampers supplied by Taylor Devices Inc, USA as described in Table 4.1.

Table 4.1. Technical specifications of fluid viscous dampers.

Sr. No.	Identification. No.	Qty	Weight (*kg*)	Stroke (*mm*)	Damper Exponent (α)	Damper Coefficient c_α (*kNs/m*)	Remarks
1	67DP-18921-01	02	82	±100	0.80	420	Type-A
2	67DP-18922-01	02	82	±100	0.36	330	Type-B

The shock parameters were measured at the damper fixed end and damper piston end. To record displacement time history of the mass and in turn displacement time history of the damper piston, a LVDT was connected between the mass and a bracket rigidly mounted on the corset platform. The data acquisition system connecting the LVDT and the sensors recorded the data for the displacement of the damper piston and the acceleration at damper fixed end and damper piston end. This data was recorded for specified shock amplitude generated by the corset striking the buffer mass with specified rubber thickness from a specified drop height and at a specified time interval. The test were conducted by using a 10 Tonne mass mounted on roller behind the damper piston end and gradually increasing the drop height (DH) from 50mm to 250mm and reducing the rubber thickness (RT) from 150mm to 50mm. The band width for measurement of shock parameters by the sensors and the displacement by LVDT used for data acquisition for all the tests conducted was set at 4096 Hz.
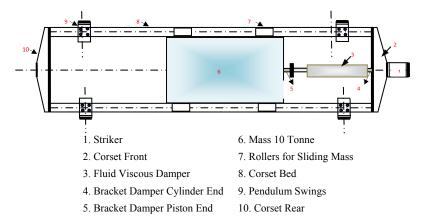

1. Striker   6. Mass 10 Tonne
2. Corset Front   7. Rollers for Sliding Mass
3. Fluid Viscous Damper   8. Corset Bed
4. Bracket Damper Cylinder End   9. Pendulum Swings
5. Bracket Damper Piston End   10. Corset Rear

Figure 4.1. Schematic of Fluid Viscous Damper mounted on corset platform of shock test facility.

4.2 Results of shock excitation on fluid viscous dampers

During the experimental program, twelve tests were performed on each of the damper Type 'A' and Type 'B'. The dampers were subjected to shock excitation for the shock generated by changing the drop height of the corset and the rubber thickness interposed between the buffer mass and a steel plate.

The noise in measured acceleration and displacement time-history data was filtered using a low pass filter process in MATLAB *Toolbox*. The cut-off frequency for filtering were manually identified using the FFT of the measured acceleration and displacement time-history, and were chosen to ensure that the response behaviour was fully represented in the filtered time-history data.

The filtered input time-history at the damper fixed end and the output time-history at the damper piston end and their corresponding shock response spectrum for one test on each of the damper are shown in Fig. 4.2. (a)-(c) for damper Type 'A' and in Figure 4.3. (a)-(c) for damper Type 'B'. It can be seen from these figures; the accelerations at the damper piston ends are considerably reduced compared to the accelerations applied at the damper fixed end, which demonstrate the ability of fluid viscous dampers to attenuate shock pulse of considerable amplitude.
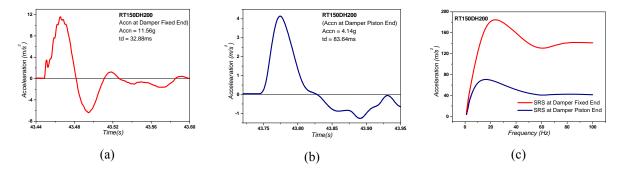

(a) (b) (c)

Figure 4.2. (a) Shock Input for Type 'A' Damper for RT150DH200, (b) Output Response for Type 'A' Damper for RT150DH200, (c) SRS of Shock Input and Output Response of Type 'A' Damper for RT150DH200
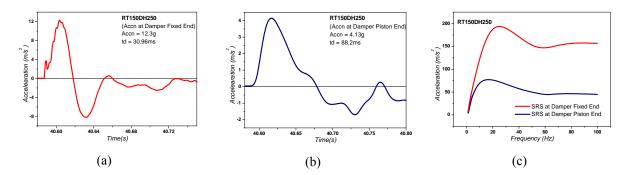

(a) (b) (c)

Figure 4.3. (a) Shock Input for Type 'B' Damper for RT150DH250, (b) Output Response for Type 'B' Damper for RT150DH250, (c) SRS of Shock Input and Output Response of Type 'B' Damper for RT150DH250

4.3 Characterisation of dampers

For the characterisation of dampers to shock excitation the sliding mass of 10 Tonne connected to the damper is assumed as a SDOF. This SDOF system is subjected to the shock excitation produced as a result of corset front striking the buffer mass from a specified height. The equation of motion for the damper mass system subjected to half-cycle sine shock $P(t)$ for a duration t_d can be written as:

For forced vibration phase:

$$m\ddot{u} + c_\alpha \dot{u}^\alpha + k_d u = P(t) ----t \le t_d \tag{4.1}$$

For free vibration phase:

$$m\ddot{u} + c_\alpha \dot{u}^\alpha + k_d u = 0 -----t \ge t_d \tag{4.2}$$

The contribution of stiffness of the damper, k_d is found to be negligible in response calculation and is not considered. The analytical response of displacement of the mass and in turn the displacement of the damper piston is calculated using the model for force-velocity as established for the sinusoidal excitation of the FVD in Eqn 1. The parameters α and c_α supplied by the manufacturer are used in the calculation of response. The analytical and the measured time-history of displacement for duration of displacement of the mass and in turn the displacement of the piston of the damper was superimposed to see, whether the force-velocity model as established for sinusoidal excitation in Eqn. 1 for the damper still remain the same for shock excitation. These superimposed graphs are as shown in the Figure 4.4. (a) for the fluid viscous damper Type 'A' and in Figure 4.4.(b) for the fluid viscous damper Type 'B'.
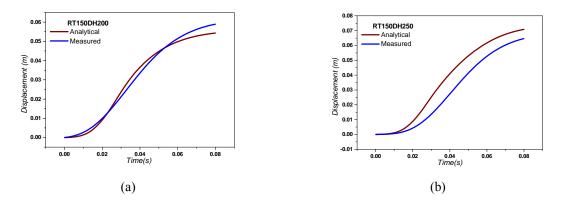

(a)   (b)

Figure 4.4. (a) Analytical and Measured Displacement Response of Type 'A' Damper for RT150DH200
(b) Analytical and Measured Displacement Response of Type 'B' Damper for RT150DH250

The following observations are made from the superposition of the analytical and the measured response of displacements.
1. The shape of the displacement time-history for the analytical and the measured response for both the damper Type 'A' and Type 'B' fairly agree indicating that the model for force-velocity as established for sinusoidal excitation still holds good for shock excitations.
2. The analytical and the measured displacements for the duration of acceleration response at the damper piston end are within a range of 10% to 20% for the nonlinear damper Type 'A' with $\alpha = 0.8$ which is very close to a linear damper. This indicates that there is no change in the damping characteristics of a nonlinear FVD very close to linear FVD in shock excitation.
3. Almost 80% of the result of superposition of the analytical and the measured response of displacement for the nonlinear damper Type 'B' shows that measured response is much lesser than the analytical response. To fit the measured response the coefficient of damper is increased in the analytical model so that the shape of the response is maintained and the difference in analytical and the measured response is within 20%. This indicates that for a highly nonlinear damper as of Type 'B' with $\alpha = 0.8$, the damping properties of the damper may be increasing under excitation. In case of use of such highly nonlinear damper, the reason for this difference needs further investigation, to eliminate the possibility of this being observed due to instrumentation or experimental setup limitation.

5. STRUCTURE WITH FVD SUBJECTED TO HALF-CYCLE SINE PULSE

5.1 Linear FVD

Considering a SDOF system equipped with linear FVD and subjected to a half- cycle sine pulse given by the Eqn. 5.1 with $t_d / T_n = 1/2$, which implies $\omega = \omega_n$ and $t_d = T_n / 2 = \pi / \omega$.

$$\ddot{u}(t) = \ddot{u}_0 \sin \omega t \tag{5.1}$$

The energy dissipated by the FVD, W_D, is given by

$$W_D = \oint F_D\, du = \oint c\dot{u}\, du = \int_0^{\pi/\omega} c\dot{u}^2\, dt \tag{5.2}$$

where F_D is the damper force, which is equal to $c\dot{u}$ for a linear FVD; c is the damping coefficient of linear FVD; and $\dot{u}$ is the relative velocity between the structure and the damper. Therefore,

$$W_D = c\frac{\dot{u}_0^2}{\omega^2} \int_0^{\pi/\omega} \left(2\sin^2\frac{\omega t}{2}\right)^2 dt \tag{5.3}$$

Let $\omega t/2 = \theta$ and $dt = 2d\theta/\omega$, Eqn. 5.3 can then be written as

$$W_D = c\left(\frac{2^3 \ddot{u}_0^2}{\omega^3}\right) \int_0^{\pi/\omega} \left(\sin^4\theta\right) dt = c\left(\frac{2^3 \ddot{u}_0^2}{\omega^3}\right) * 0.58905 \tag{5.4}$$

The damping ratio contributed by the linear FVD can be expressed as $\xi_{sd} = c/c_{cr}$. Therefore, Eqn. 5.4 can be written as:

$$W_D = 2^4 m\omega_n \xi_{sd} \left(\frac{\ddot{u}_0^2}{\omega^3}\right) * 0.58905 \tag{5.5}$$

5.2 Nonlinear FVD

Considering a SDOF system equipped with nonlinear FVD and subjected to a half-cycle sine pulse given by the Eqn. 5.1 with $t_d/T_n = 1/2$, which implies $\omega = \omega_n$ and $t_d = T_n/2 = \pi/\omega$. The energy dissipated by the FVD, W_D, is

$$W_D = \oint c_\alpha \dot{u}\dot{u}^\alpha\, du = \int_0^{\pi/\omega} \left|c_\alpha \dot{u}^{1+\alpha}\right| dt \tag{5.6}$$

$$W_D = c_\alpha \frac{\dot{u}_0^{1+\alpha}}{\omega^{1+\alpha}} \int_0^{\pi/\omega} \left|\left(2\sin^2\frac{\omega t}{2}\right)^{1+\alpha}\right| dt \tag{5.7}$$

Let $\omega t/2 = \theta$ and $dt = 2d\theta/\omega$, Eqn. 5.7 can then be written as follows:

$$W_D = c_\alpha \frac{\ddot{u}_0^{1+\alpha}}{\omega^{2+\alpha}} 2^{2+\alpha} \int_0^{\pi/2} \left(\sin^{2+2\alpha}\theta \cos^0\theta\right) dt \tag{5.8}$$

$$W_D = c_\alpha \frac{\ddot{u}_0^{1+\alpha}}{\omega^{2+\alpha}} 2^{2+\alpha} * \frac{\Gamma(\alpha+3/2)\Gamma(1/2)}{2\Gamma(\alpha+2)} \tag{5.9}$$

where Γ is the gamma function. The energy dissipated is thus expressed as follows:

$$W_D = c_\alpha \frac{\ddot{u}_0^{1+\alpha}}{\omega^{2+\alpha}} 2^{2+\alpha} * \psi \tag{5.10}$$

The nonlinear and linear FVDs dissipate an equal amount of energy for a SDOF system subjected to

half-cycle sine pulse excitation. Therefore, equating Eqn. 5.5 and Eqn. 5.10 we obtain:

$$c_\alpha = 2\xi_{sd} m\omega_n \frac{\ddot{u}_0^{1-\alpha}}{\omega^{1-\alpha}} \left(\frac{2^{1-\alpha} \times 0.58905}{\psi} \right) \tag{5.9}$$

$$c_\alpha = 2\xi_{sd} m\omega_n \frac{\ddot{u}_0^{1-\alpha}}{\omega^{1-\alpha}} \times \kappa \tag{5.10}$$

For a linear fluid viscous damper, $\alpha=1$ and $\kappa=0.58905$, and Eqn. 5.10 reduces to:

$$c = 2\xi_{sd} m\omega_n \tag{5.11}$$

6. EQUATIONS OF MOTION

The equation of motion for a SDOF system with mass m equipped with a non-linear FVD, and subjected to a half-cycle sine pulse $p(t) = p_0 \sin \omega t$, is:

$$m\ddot{u} + c\dot{u} + ku + c_\alpha \, \text{sgn}(\dot{u})|\dot{u}|^\alpha = p_0 sin\omega t \tag{6.1}$$

or,

$$\ddot{u} + 2\xi\omega_n\dot{u} + \omega_n^2 u + \frac{c_\alpha}{m}\text{sgn}(\dot{u})|\dot{u}|^\alpha = \ddot{u}_0 Sin\omega t \tag{6.2}$$

In these equations, α is the damper exponent and c_α is the damping coefficient, while the over dots represent derivatives with respect to time. The natural frequency of the structure is given by $\omega_n = \sqrt{k/m}$ and ξ is the natural damping ratio. When c_α is non-zero and $\alpha \neq 1$, Eqn. 6.2 becomes nonlinear; therefore, the response u of the system depends nonlinearly on the excitation intensity $\ddot{u}(t)$.

7. DESIGN CHARTS OF SHOCK RESPONSE SPECTRUM

The structural designer is usually interested in the maximum response quantities like displacement u_0, damper force f_0, lateral resisting force r_0, and time of maximum response t_0. Here, the design charts for maximum response of SDOF system without and with FVDs subjected to half- cycle sine pulse are presented in Fig. 7.1. These charts provide results for maximum non-dimensional displacement, damper force, and the time of maximum response. The maximum lateral resisting force r_0 can be evaluating by knowing the maximum displacement u_0 and the stiffness k of the structure.

7.1. Example System

To illustrate the use of charts as shown in Fig. 7.1., consider the SDOF system in Fig. 7.2. is subjected to a half-cycle sine pulse as shown in Fig. 7.3. It is observed from Table 7.1. that the nonlinear FVD requires much lower supplemental damping and hence much smaller damping coefficient than the linear FVD for approximately the same values of peak responses for the given shock loading. The lower value of supplemental damping or the coefficient of damper means a much lower and compact size of nonlinear fluid viscous damper. Thus, knowing the natural period of the structure T_n and the duration t_d of the pulse shock, one can estimate the maximum displacement, amount of damping force on the system by the added linear $\alpha = 1$ or nonlinear $\alpha < 1$ FVD for a particular value of supplemental damping. It thus become easier for a designer to choose a most suitable nonlinear fluid viscous damper for the design of structural system with appropriate damper exponent α and damping coefficient c_α for a given pulse shock from the design charts.
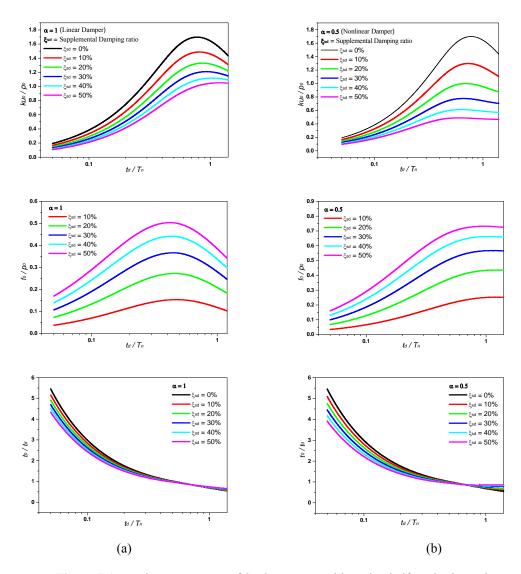
Figure 7.1. Maximum response of SDOF system subjected to half-cycle sine pulse.
(a) Linear FVD ($\alpha = 1$), and (b) Nonlinear FVD ($\alpha = 0.5$)

Example SDOF system parameters:

Mass (m) = 25000 kg

Stiffness (k) = 9869×10^3 kN/m

Natural Period $T_n = 0.01$ s

Structural damping $\xi = 2\%$

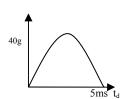**Figure 7.2.** Schematic diagram of SDOF system.

Figure 7.3. Half-cycle sine pulse

Table 7.1. Peak responses of SDOF system.

Maximum Response Quantity	Without FVD	Linear FVD ($\alpha = 1$)	Nonlinear FVD ($\alpha = 0.5$)
Displacement u_0 (mm)	1.5242	1.032	0.7497
Lateral Resisting Force r_0 (kN)	15042.33	10184.81	7398.79
Damper Force f_0 (kN)	-	3580.65	4991.33
Time of maximum response t_0 (ms)	5	4.9	4.8
Supplemental Damping Ratio ξ_{sd} (%)	-	30	30
Coefficient of Damper c_α (kNs/m)	-	9424.78	9306.90

For the example SDOF system, $t_d / T_n = 0.5$. The maximum responses of example SDOF system without and with linear fluid damper ($\alpha = 1$) and nonlinear fluid damper ($\alpha = 0.5$) are found out using the response charts as shown in Fig. 7.1. These responses are tabulated in Table 7.1.

8. CONCLUSIONS

From the discussions presented in this paper, the following conclusions can be drawn:
1. The force-velocity model as verified in sinusoidal excitation is found to be valid when the fluid viscous dampers are subjected to shock excitation. It is found that the damping properties of the nonlinear damper close to a linear damper subjected to shock excitation almost remain the same as in the sinusoidal excitation. However, the damping properties of a much nonlinear damper subjected to shock excitation are found to be considerably increased especially for shock pulse of larger magnitude and of shorter duration.
2. For the same values of peak responses for the given shock loading the coefficient of damper for a nonlinear fluid viscous damper is much smaller than the linear fluid viscous damper indicating a much smaller and compact size of damper.
3. The displacement and velocity decay at a much faster rate with the use of nonlinear dampers. This property can be utilized to improve the reliability of secondary systems mounted on the structure.
4. Design charts can serve as a ready reference for the structural designer to choose the most appropriate nonlinear damper with suitable damper exponent and coefficient of damping for a particular half-sine pulse shock.

REFERENCES

Constantinou, M. C. and Symans, M. D. (1992). Experimental and analytical investigation of seismic response of structures with supplemental fluid viscous dampers. Report No. NCEER- 92-0032, National Center for Earthquake Engineering Research, Buffalo, NY, USA.
Constantinou, M. C. and Symans, M. D. (1993). Seismic response of structures with supplemental damping, *The Strucural Design of Tall Buildings*, **2**, 77-92.
Dicleli, M. and Mehta, A. (2007). Effect of near-fault ground motion and damper characteristics on the seismic performance of chevron braced steel frames, *Earthquake Engineering Structural Dynamics*. **36**, 927-948.
Goel, R. K. (2005). Seismic response of linear and non-linear asymmetric systems with nonlinear viscous dampers, *Earthquake Engineering Structural Dynamics*. **34**, 825-846.
Harris, C. M. and Crede, C. E. (1961), *Shock and Vibration Handbook*, McGraw-Hill Inc, New York, NY, USA.
Lin, W. H. and Chopra, A. K. (2002). Earthquake response of elastic SDF system with non-linear fluid viscous dampers, *Earthquake Engineering Structural Dynamics*. **31**, 1623-1642.
Makris, N. (1992). Theoretical and experimental investigation of viscous dampers in applications of seismic and vibration isolation. Ph.D. Thesis, State University of New York at Buffalo, NY, USA.
Martinez-Rodrigo, M. and Romero, M. L. (2003). An optimum retrofit strategy for moment resisting frames with non- linear viscous dampers for seismic applications, *Engineering Structures*. **25,** 93-132.
Peckan, G., Mander, J. B. and Chen, S. S. (1999). Fundamental considerations for the design of non-linear viscous dampers, *Earthquake Engineering Structural Dynamics*. **28**, 1405-1425.
Soong, T. T. and Dargush, G. F. (1997), *Passive Energy Dissipation Systems in Structural Engineering*, Wiley: New York.